





# $2 \times 300$ Gbit/s Line Rate PS-64QAM-OFDM THz Photonic-Wireless Transmission

Shi Jia , Lu Zhang , Shiwei Wang , Wei Li, Mengyao Qiao , Zijie Lu, Nazar Muhammad Idrees , Xiaodan Pang , *Senior Member, IEEE*, Hao Hu , Xianmin Zhang , Leif K. Oxenløwe, and Xianbin Yu , *Senior Member, IEEE*

**Abstract**—The proliferation of wireless broadband services have significantly raised the demand for high data rates. Due to the limited bandwidth of radio frequency (RF) bands that are currently in use for communication purposes, the choice of the ‘Terahertz (THz) frequency region’ (0.3–10 THz) is getting favored thanks to its merits of bringing together wireless and optical communications with photonics technologies. We report on an experimental demonstration of a hybrid THz photonic-wireless transmission based on a THz orthogonal polarization dual-antenna scheme. Probabilistic shaped 64-ary quadrature amplitude modulation based orthogonal frequency division multiplexing (64QAM-OFDM) modulation format is used to realize high transmission rate. A potential total system throughput of 612.65 Gbit/s (around  $2 \times 300$  Gbit/s line rate) with an average net spectral efficiency of 4.445 bit/s/Hz per antenna is successfully achieved.

**Index Terms**—Radio-frequency photonics, THz communication, ultrafast information processing.

Manuscript received December 29, 2019; revised April 3, 2020 and May 13, 2020; accepted May 16, 2020. Date of publication May 19, 2020; date of current version September 1, 2020. This work was supported in part by the National Key Research and Development Program of China (2018YFB1801500 and 2018YFB2201700), in part by the Natural National Science Foundation of China under Grant 61771424, in part by the Natural Science Foundation of Zhejiang Province under Grant LZ18F010001, in part by the European Horizon 2020 research and innovation program under the Marie Skłodowska-Curie grant agreement No. 713683 (COFUNDfellowsDTU), in part by the Danish centre of excellence CoE SPOC under Grant DNR123, in part by the Villum young investigator program under Grant 2MAC, in part by the Independent Research Fund Denmark under the grant of 9041-00395B, in part by the Swedish Research Council (VR) under Grant 2019-05197, and in part by the Fundamental Research Funds for the Central Universities. (*Corresponding authors: Xianbin Yu; Shi Jia.*)

Shi Jia is with the College of Information Science and Electronic Engineering, Zhejiang University, Hangzhou 310027, China, and also with the DTU Fotonik, Department of Photonics Engineering, Technical University of Denmark DK-2800, Kgs. Lyngby, Denmark (e-mail: shijai@fotonik.dtu.dk).

Lu Zhang and Xianbin Yu are with the College of Information Science and Electronic Engineering, Zhejiang University, Hangzhou 310027, China, and also both with the Zhejiang Lab, Hangzhou 310000, China (e-mail: zhanglu1993@zju.edu.cn; xyu@zju.edu.cn).

Shiwei Wang, Wei Li, Mengyao Qiao, Zijie Lu, Nazar Muhammad Idrees, and Xianmin Zhang are with the College of Information Science and Electronic Engineering, Zhejiang University, Hangzhou 310027, China (e-mail: wsw@zju.edu.cn; lwecei@zju.edu.cn; qiaomy@zju.edu.cn; luzijie@zju.edu.cn; nazar@zju.edu.cn; zhangxm@zju.edu.cn).

Hao Hu and Leif K. Oxenløwe are with the DTU Fotonik, Department of Photonics Engineering, Technical University of Denmark, DK-2800 Kgs. Lyngby, Denmark (e-mail: huhao@fotonik.dtu.dk; lkox@fotonik.dtu.dk).

Xiaodan Pang is with the Applied Physics Department, KTH Royal Institute of Technology, 164 40 Kista, Sweden (e-mail: xiaodan@kth.se).

Color versions of one or more of the figures in this article are available online at <https://ieeexplore.ieee.org>.

Digital Object Identifier 10.1109/JLT.2020.2995702

## I. INTRODUCTION

WITH the ever-expanding degree of digitalization of our society, the past few years have witnessed an astounding annual growth of the mobile data traffic around 50% [1]. To face the challenges brought by the coming or emerging 5G, beyond 5G (B5G) and Internet of Things (IoT) services, the demand for wireless bandwidth and data traffic is projected to grow even faster in the coming years [2]–[4]. Capacity crunch is becoming a major challenge for current and future wireless communication networks, as the incremental connection speed provided by moving from 3G to 5G networks may not be sufficient to meet all requirements. Therefore, higher data rates beyond 100 Gbit/s, and eventually Tbit/s scale, are predicted to be required in numerous wireless connections [5], [6].

As of today, the spectral resources in the frequency range below 60 GHz have been almost fully exploited and are limited by the transmitted power [7]. Subsequently, the unexploited higher frequency bands providing larger bandwidth are currently being explored for wireless communications [7]. The development of photonics technologies has significantly accelerated the research progress to demonstrate very high data rate transmission in frequency bands above 60 GHz, with heterodyne photo-mixing, which becomes an attractive solution for transparent millimeter wave (MMW) and THz signal generation [8], [9]. In details, photo-mixing based photonics technique, on one hand, features the capability of generate broadband MMW/THz signals with frequency tunability by overcoming the electronic bandwidth bottle neck. On the other hand, it is also transparent to optical modulation formats, which enables a unique opportunity to transfer large optical capacity into the wireless domain, and provides a promising solution to seamlessly converge the fiber-optic networks and wireless networks for future generations. In the W-band (75–110 GHz), several works incorporating spatial multiple-input-multiple-output (MIMO) and optical polarization division multiplexing (PDM) techniques [10]–[14] of data rates in the order of 100 Gbit/s have been demonstrated. In the D-band (110–170 GHz), a record of delivering up to 1-Tbit/s capacity has been realized by using MIMO and probabilistic shaping 64-ary quadrature amplitude modulation (PS-64QAM) [15]. System-level demonstrations in the sub-THz band (200–300 GHz), with the wireless data rates in the order of 100 Gbit/s, have also been demonstrated by employing uni-travelling photodiodes (UTC-PDs) and optical frequency comb sources

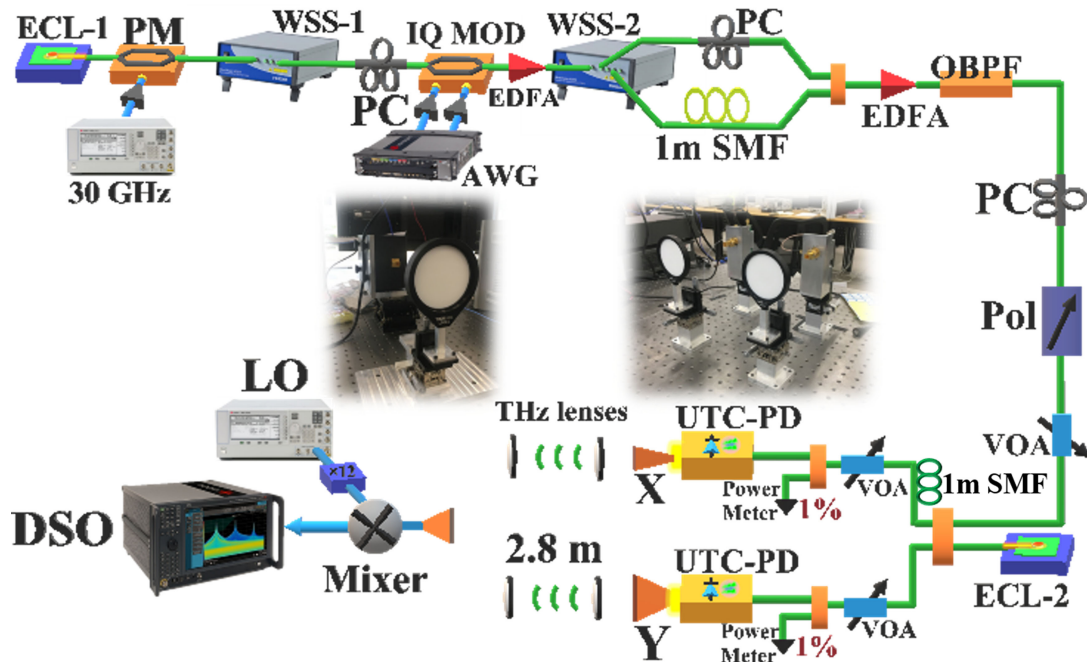


Fig. 1. Experimental setup of the 320-380 GHz communication link. ECL: external cavity laser; PM: phase modulator; WSS: wavelength selective switch; PC: polarization controller; IQ MOD: IQ modulator; AWG: arbitrary waveform generator; EDFA: erbium-doped fiber amplifier; SMF: single-mode fiber; OBPF: optical band-pass filter; Pol.: polarizer; VOA: variable optical attenuator; UTC-PD: uni-travelling carrier photodiode; LO: local oscillator; DSO: digital sampling oscilloscope. The insets: the pictures of the actual UTC-PDs, THz receiver and THz lenses at the corresponding transmitter and receiver sides respectively.

[16]–[18]. To approach the next wireless data rate milestone of Tbit/s, exploration of the THz band (above 300 GHz) seems mandatory, since much wider unallocated bandwidth is available. Following this trend, several wireless transmission links operating in the THz region have been proposed and demonstrated [19]–[37]. The recent record of 260 Gbit/s wireless data rate has been achieved by utilizing multi-channel Nyquist 16-ary quadrature amplitude modulation (QAM) in the 325-475 GHz band [38]. However, due to the low spectral efficiency of 1.73 bit/s/Hz, limited bandwidth of the THz down-conversion receiver and the poor frequency response of the optical/THz channel, the demonstrated data rate in [38] is still far below the targeted Tbit/s milestone. Thus, the use of higher order modulation formats and optimized spectral arrangement over the occupied frequency band is essential as a way forward.

In this paper, we propose and verify a new approach to utilize the bandwidth in the THz region more efficiently. Our proposed THz photonic-wireless transmission scheme is experimentally demonstrated with a record high line rate of 612.65 Gbit/s (around  $2 \times 300$  Gbit/s line rate and  $2 \times 250$  Gbit/s net rate) operating in the 320-380 GHz band with the high spectral efficiency of 4.445 bit/s/Hz per polarization. Firstly, a highly spectrally efficient modulation format of 64QAM combining with orthogonal frequency-division multiplexing (OFDM) and probabilistic shaping (PS) is employed, named as PS-64QAM-OFDM. Secondly, a THz transmitter based on THz orthogonal polarization dual antenna scheme allows to further improve the spectral efficiency doubles the system capacity. Thirdly, a key component enabling the THz signal with high signal-to-noise ratio (SNR) providing more highly spectrally efficient modulation format is the photo-mixer implemented with a uni-traveling

carrier photodiode (UTC-PD) with higher conversion efficiency. Such a photo-mixer satisfies the strong requirements in terms of broad bandwidth, high responsivity and high output power. Finally, we use channel post-equalization digital signal processing (DSP) routine to recover the transmitted data. The bit error rate (BER) performance of the demonstrated system is successfully achieved below the low-density parity-check convolutional codes (LDPC-CC) FEC threshold ( $2.7E-2$ , 20%-OH) limit over 2.8 m wireless distance and reaching a record data rate.

This paper is organized as follows. In Section II, we present the details of our experimental configuration with an emphasis on the high-speed optical baseband modulation followed by optical local oscillator combining, THz emission, transmission and reception, and the DSP routine. Section III shows the experimental results and gives the corresponding discussions. Finally, the conclusions are drawn in Section IV.

## II. EXPERIMENTAL CONFIGURATION

### A. The High-Speed Optical Baseband Modulation and Optical Local Oscillator Combining

The experimental configuration is shown in Fig. 1. A continuous wave (CW) light centered around 1550 nm and an output power of around 15.5 dBm from an external cavity laser (ECL-1, <100 kHz linewidth), is launched into a phase modulator (PM, 40 GHz bandwidth) to generate a coherent optical frequency comb (OFC). The PM is driven by a 30 GHz RF sinusoidal signal of 20 dBm for 2-carrier operation, which determines the comb line spacing. After the PM, the generated OFC with 30 GHz line spacing is fed into a wavelength selective switch (WSS-1, Finisar WaveShaper 4000S). WSS-1 is used to

select two neighboring phase-locked comb slots to be used as optical carriers and perform power equalization. At the output of the WSS-1, the two selected coherent optical carrier tones are launched into an in-phase (I) and quadrature (Q) optical modulator (IQ-MOD, 40 GHz bandwidth), where a polarization controller (PC) is used to align the polarization of optical carriers with the IQ-MOD. A two-channel 65 GSa/s arbitrary waveform generator (AWG, Keysight M8195A, 25 GHz analog bandwidth, 8 bits vertical resolution) is used to generate the PS-64QAM-OFDM signal and drive the IQ-MOD. The length of the inverse fast Fourier transform (IFFT) and cyclic prefix (CP) of the PS-64QAM-OFDM signal are set to 1024 and 16, respectively, and the first two subcarriers are set to null. The OFDM signal is formed from a random bit sequence generated from MATLAB. The sequence length depends on the spectral efficiency and the number of OFDM symbols. In the experiment, there are 150 OFDM symbols and the pattern length is around  $8.5E5$  bits. The data length of OFDM signal is around  $1.56E5$  samples, and the pseudo random sequence is inserted for frame synchronization. After modulation and being amplified by an erbium-doped fiber amplifier (EDFA), the two optical baseband channels are separated by WSS-2. A 1-m fiber based delay line is added in one path to de-correlate the signals between the two adjacent channels. The gain of EDFA before the WSS-2 is variable to preserve the WSS from being damaged by excessive input power. Then two modulated optical tones are aligned by a PC to adjust the polarization state. Then, they are combined by a 3-dB optical coupler and amplified by an EDFA followed by an optical band-pass filter (OBPF) to suppress out-of-band amplified spontaneous emission (ASE). A second free-running ECL (ECL-2, ID Photonics CoBriteDX1), acting as a remote optical local oscillator (LO), is coupled with the modulated optical signal after the polarization alignment by a PC and polarizer for the THz signal generation. Here, a polarization maintaining (Pol. M) variable optical attenuator (VOA) is used to control the power of the optical signal with modulation before combining the optical LO, to keep the power ratio balanced between the optical LO and signal for the highest photo-mixing efficiency in the uni-travelling carrier photodiode (UTC-PD) [39].

### B. THz Emission, Transmission and Reception

The combined optical modulated signal and un-modulated LO are divided into two equal parts by a 3-dB Pol. M coupler, which are sent into two corresponding ultra-broadband UTC-PDs (IOD-PMJ-13001) respectively for the heterodyne photomixing-based generation of THz signals [40]. It should be noted that the length difference between the two optical paths from the coupler to UTC-PD-X and -Y is set to longer than 1m, and hence the signals launched into two UTC-PDs are de-correlated. Before each UTC-PD, there is a Pol. M VOA used to control the launched optical power, which is up to 13 dBm. The THz output power of the UTC-PD (280–380 GHz, 100 GHz bandwidth) with a conversion efficiency of 0.15 A/W is from  $-20$  dBm to  $-10$  dBm, depending on the optical input power. The THz rectangle horn antennas after the UTC-PDs are used to radiate generated THz waves and control the polarization

of the emitted THz beams by rotating the antennas around their horizontal central axis. In this experiment, the longer side of rectangular opening of one THz horn antenna is along the horizontal axis X, as the longer side of the other antenna is along the vertical axis Y in order to avoid the polarization crosstalk between the two THz antennas, as shown in the insets of Fig. 1. At the output of each UTC-PD followed by a horn antenna, dual-channel THz signals with corresponding polarization are generated and emitted into the free space. Two pairs of THz lenses with a 100-mm diameter and 200-mm focus length are employed to collimate the THz beams in two 2.8-m line-of-sight (LOS) links corresponding to the X and Y antennas respectively (as shown in the insets of Fig. 1).

At the receiver side, in each polarization path, the received THz signal in each channel is individually down-converted to an intermediate frequency (IF) signal, by using a sub-harmonic Schottky mixer (VDI WR2.2, 40 GHz IF bandwidth) operating in the 320–500 GHz band. The mixer is driven by a 12-time frequency multiplied electrical LO signal, which is tunable in the frequency range of 26.7–31.7 GHz. It should be noted that here we use one single THz receiver to successively receive and down-convert the THz signals from the X path and Y path. The transmitted THz signals in X and Y path can be received and down-converted simultaneously in theory when the experiment condition is satisfied. In the experiment, the 60-GHz available data bandwidth is equally separated into two 30-GHz channels which are down-converted individually at the receiver side, which is limited by the data bandwidth of the AWG and IF bandwidth of the THz receiver. However, it should be noted that the current all-electrical processing capability of data signal generation, receive and de-modulation could cover 60-GHz bandwidth. Therefore, if we employ the AWG and THz receiver with wider bandwidth, the 60-GHz data signal can be generated, received and down-converted simultaneously instead of two channels.

The IF output is amplified by a RF amplifier with 22-dB gain and 60-GHz bandwidth, and then sent into a broadband real-time digital sampling oscilloscope (DSO, Keysight DSOZ594A Infiniium, 8 bits vertical resolution) with 160 GSa/s sampling rate and 59 GHz analogue bandwidth for analog-to-digital conversion. The data length collected in the receiver depends on the storage space of the DSO, it is set to  $4E6$  in the experiment, and the OFDM signal frame is extracted after synchronization.

### C. Digital Signal Processing (DSP) Routine

At the transmitter side, the PS method [41] is used to map the bit sequence to PS-64QAM symbols, where each axis of the 64QAM constellations is distributed based on Maxwell-Boltzmann distribution. The probability mass function of in-phase and quadrature-phase symbol of QAM is shown as follows.

$$P_X(x_i) = k * \exp(-v|x_i|^2). \quad (1)$$

$$k = 1/\sum_{j=1toM} \exp(-v|x_j|^2). \quad (2)$$



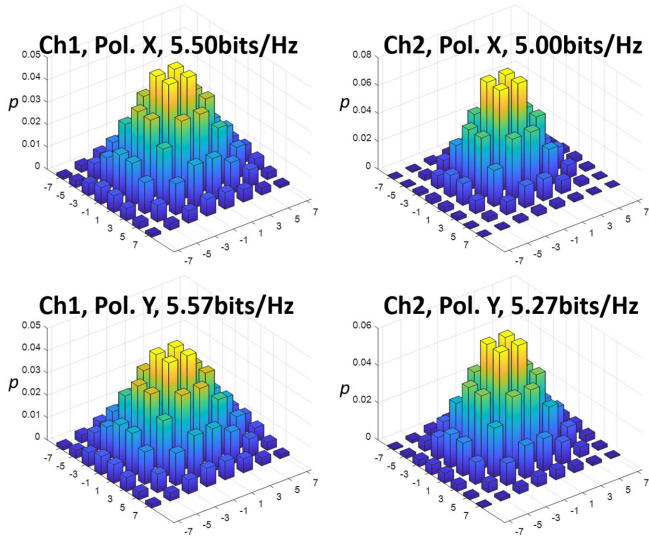


Fig. 2. The 64-QAM constellation probability distributions of different carriers in different paths.

The symbol  $x_i$  means the discrete symbol of in-phase and quadrature-phase symbol of QAM, it corresponds to  $\{-7, -5, -3, -1, +1, +3, +5, +7\}$  for 64QAM mapping. The variable  $v$  in the range of  $[0, 1]$  is used to control the shape of the probability distribution. Larger  $v$  will contribute to larger variance of the probabilities at different symbols, it is adjusted in the experiment according to the channel SNR. The variable  $k$  is used to keep the addition of all probabilities equals to 1. As the probabilistic shaping technique applies a higher probability to the inner constellation points, and a lower probability to the outer constellation points, resulting in a reduced average power compared to the equally distributed 64-QAM signals. Therefore, an improved noise tolerance and a better bit-energy efficiency in a transmission system can be expected. The 64-QAM constellation probability distributions of different carriers in different paths here is shown in Fig. 2. After subcarrier mapping, the IFFT module realizes the OFDM modulation and CP is used to reduce the influence of inter-symbol interference.

At the receiver side, the DSP equalization routine is shown in Fig. 3. The signal is first down-converted from IF to the baseband and synchronized. Then, FFT module carries out the OFDM demodulation after CP removal. After that, post-equalization is used to mitigate the channel impairments. The channel post-equalization is composed of linear equalization (LE), phase noise compensation (PNC) and nonlinear equalization (NE) modules. The LE pilots are interleaved in the time domain, and the linear channel response of each subcarrier is estimated by averaging the pilot response at the corresponding subcarriers. Then, the signals in the frequency domain are compensated by the least-squares algorithm [42]. After the LE, the signal is re-modulated to the time domain by the IFFT operation and the phase noise is compensated in the time domain by linear interpolation-based fitting process [33]. In the final step, the OFDM signal in the time domain is equalized with the Volterra

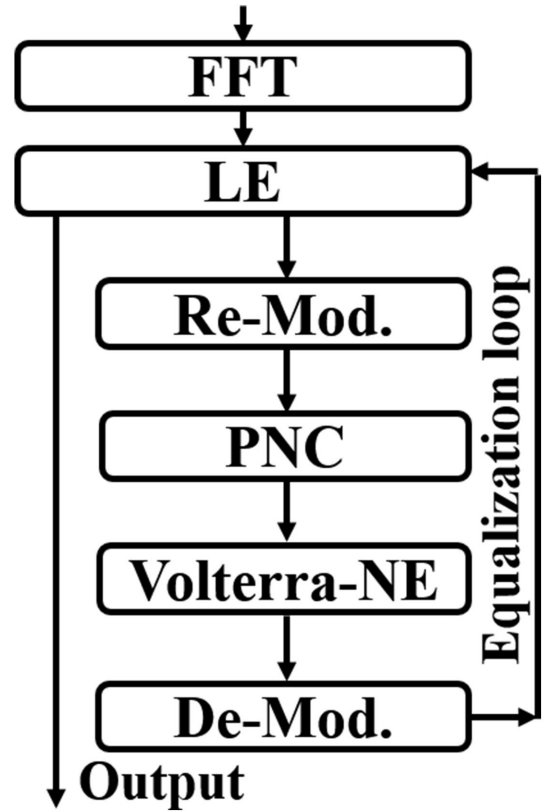


Fig. 3. DSP equalization routine at the receiver side.

filtering to mitigate the nonlinear impairments [43]. In the experiment, nonlinear Volterra kernels up to 3rd order are considered, and the recursive least squares (RLS) algorithm [43] is used for the coefficients training. After the Volterra filtering, the signal is recovered back to the frequency domain by the FFT operation. The user data is recovered back by QAM de-mapping when the iteration loop ends. The channel post-equalization is an iterative process, where the NE occupies most of the computational complexity. Assuming the iteration number is  $N_I$ ,  $M_k$  is the memory length of  $k$ -th order Volterra kernel, the complexity is in the order of  $O(N_I \cdot M_k^3)$ . In the experiment, the iteration number  $N_I$  is set to 3 and the memory length of 2nd Volterra kernel  $M_2$  and 3rd Volterra kernel  $M_3$  are set to 11 and 9, respectively.

### III. RESULTS AND DISCUSSIONS

As illustrated in Fig. 4(a), the combined optical spectrum consisting of one un-modulated optical LO tone and two-channel optical carriers with modulation before being launched into the UTC-PD, is measured by an optical spectrum analyzer (OSA, APEX AP206x) with high resolution (140 MHz/1.12 pm). The photo-mixing of the LO laser and modulated carriers in the UTC-PD generates two-channel THz signals. The combined electrical spectrums of the generated THz signals in X and Y paths are shown in Fig. 4(b) and Fig. 4(c), measured from the down-converted IF signal after 2.8 m wireless transmission. As shown in Fig. 4(b), the signal can be successfully received

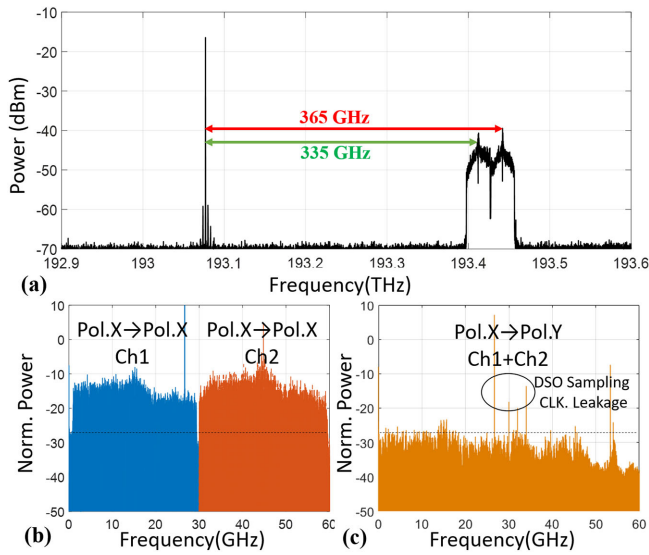


Fig. 4. (a) The optical spectrum of combing modulation and LO wavelengths. The combined THz electrical spectrum in one path (X polarization) when (b) aligned with the polarization state of the receiver (Pol. X→Pol.X), and (c) perpendicular to the polarization state of the receiver (Pol. X→Pol.Y).

when the antenna polarization axis is aligned with the receiver side. Comparatively, there is no useful signal when the receiver polarization is perpendicular to that of the transmitter, as shown in Fig. 4(c). Therefore, there is negligible polarization crosstalk between X and Y paths, confirming the feasibility of multiplexing THz polarizations in our experimental demonstration. In the electrical spectrum, only the frequency tones which are higher than the background noise in the DSO clock leakage is observed. The operational bandwidth of the THz link in this work is basically limited by the UTC-PD (280–380 GHz) and the THz receiver (320–500 GHz), which lead to the only 60 GHz (320–380 GHz) available bandwidth. Furthermore, the limitation of the system performance is basically from the SNRs of the received THz signals and the un-even frequency response over the THz receiver’s bandwidth. In terms of the SNR, the conversion efficiency of the UTC-PD (0.15 A/W) and the THz receiver are the primary limiting factors. In terms of the latter, the un-even frequency response further results in lower SNRs for the outer THz spectrum, as shown in the received THz signals spectrum in Fig. 4.

The two-channel THz signals in both X and Y paths are evaluated after the 2.8-m wireless transmissions. The bit error ratio (BER) performance is measured as a function of the launched optical power into the UTC-PDs for each channel for both two paths with orthogonal THz polarizations (X and Y). The measured BER performance is shown in Fig. 5. Here we use the low-density parity-check convolutional codes (LDPC-CC) FEC threshold ( $2.7E-2$ , 20%- OH) [33]. It can be seen that both transmissions through the two THz polarization multiplexing paths can reach the FEC threshold at optical powers of 12 to 13 dBm, respectively. The line rate of the first and second channel of the X polarization are 155.01 Gbit/s and 146.63 Gbit/s, respectively. Similarly, the line rate of the first and second channel of the Y polarization are 159.81 Gbit/s and 151.20

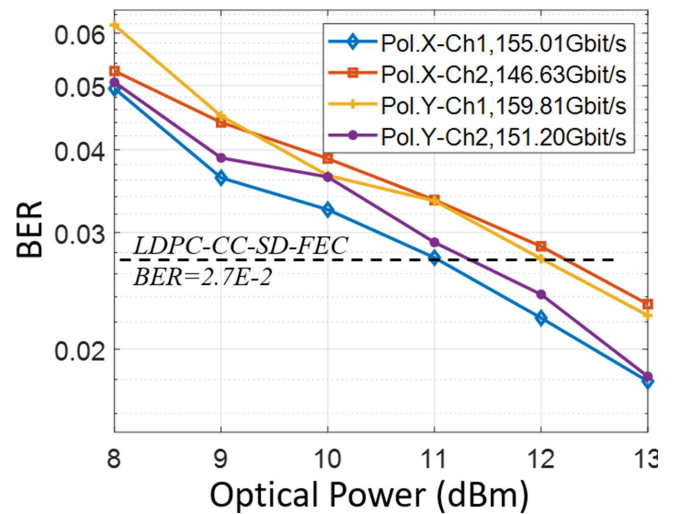


Fig. 5. BER performance versus the optical power launched into the UTC-PD for two channels for X path and Y path.

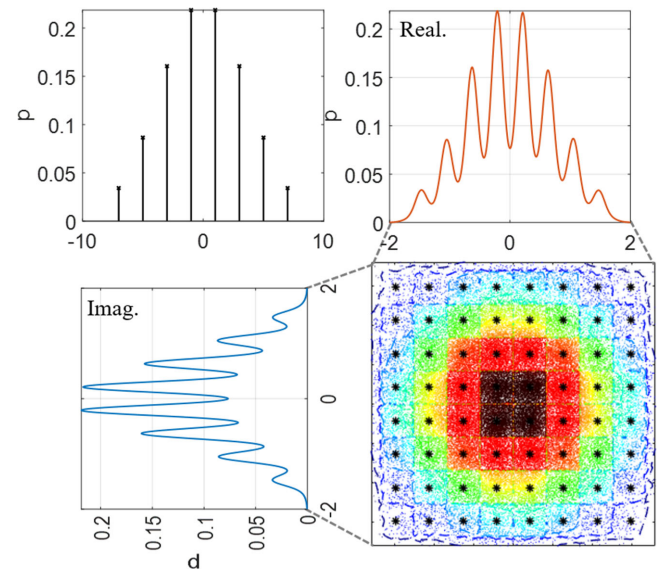


Fig. 6. Constellations captured at an optical power of 13 dBm for each channel for both two paths.

Gbit/s, respectively. In this case, the potential total system line rate is up to 612.65 Gbit/s, resulting in a net rate of 510.5 Gbit/s and an average net spectral efficiency of 4.445 bit/s/Hz per polarization, when subtracting the FEC overhead. The PS-64QAM constellation with 5.5 bit/symbol PS efficiency at 13 dBm optical power for the first channel of the X path is shown in Fig. 6. The constellation points are marked according to their probability distribution density, and the probability mass function of in-phase and quadrature-phase symbol of transmitted and received PS-64QAM are also shown in the insets of Fig. 6. As shown in Fig. 7, the BER performance for the first channel of X path for four cases of different DSP modules combined (w/o equalization, LE, LE+PNC, LE+PNC+NE), has been measured as a function of the optical power launched into the UTC-PD. It shows the BER performance improvement by using

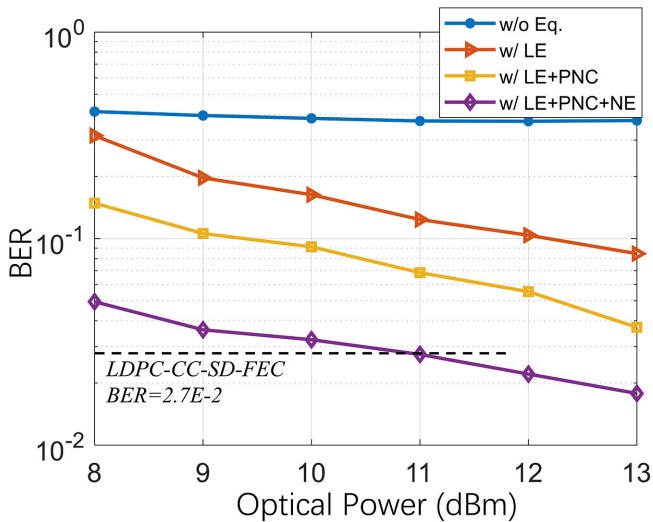


Fig. 7. BER versus the optical power launched into the UTC-PD, for the first channel of X path, for 4 cases with different combinations of DSP modules.

the DSP algorithms. In addition, it is noted that the technique of OFDM is employed together with PS-64QAM in this experiment, to minimize the influence of un-flat frequency response and especially the harmonic spurs within the bandwidth of the THz receiver.

It should be noted that here we use two polarization orthogonal THz antennas to double the system capacity, which is different from the current MIMO technology. Most of the MIMO systems currently in use transmit same copies of signal with phase differences / time delays to all the antenna elements for beamforming and use space-time coding to mitigate multipath effect. However, this is different from spatial/polarization multiplexing that we are exploring in this work. In our case, considering our very high data rate and sufficient time delay that is longer than the memory length of our receiver, this wireless system can be regarded as two independent data channels (X and Y paths). Moreover, we have detected each polarization path blindly and independently without any space-time decoding. Therefore, this is intrinsically different from the current MIMO technology. In the future, according to [44], it is well envisioned that the spatial multiplexing and beamforming can be converged in a single ultra-massive MIMO system: 1) divide the whole antenna array into sub-arrays; 2) each sub-array transmitting independent data; 3) within each sub-array one can perform beamforming.

#### IV. CONCLUSION

We have proposed and experimentally demonstrated a THz photonic-wireless transmission system in the 320–380 GHz band with an extremely high line rate of 612.65 Gbit/s (approximately  $2 \times 300$  Gbit/s line rate and  $2 \times 250$  Gbit/s net rate) and an average net spectral efficiency of 4.445 bit/s/Hz per antenna. The THz photonic-wireless transmission system with such a high bitrate is enabled by employing PS-64QAM-OFDM modulation, THz orthogonal polarization dual antenna-based reception scheme and specifically tailored post-equalization DSP routine.

#### REFERENCES

- [1] Mar. 9, 2020. [Online]. Available: <https://www.cisco.com/c/en/us/solutions/collateral/executive-perspectives/annual-internet-report/white-paper-c11-741490.html>
- [2] Y. Niu, Y. Li, D. Jin, L. Su, and A. V. Vasilakos, "A survey of millimeter wave communications (mmWave) for 5G: Opportunities and challenges," *Wireless Netw.*, vol. 21, pp. 2657–2676, 2015.
- [3] T. S. Rappaport *et al.*, "Millimeter wave mobile communications for 5G cellular: It will work," *IEEE Access*, vol. 1, pp. 335–349, 2013.
- [4] T. Wang *et al.*, "Spectrum analysis and regulations for 5G," in *Proc. 5G Mobile Commun.*, 2017, pp. 27–50.
- [5] T. Nagatsuma, G. Ducournau, and C. C. Renaud, "Advances in terahertz communications accelerated by photonics," *Nat. Photon.*, vol. 10, no. 6, pp. 371–379, Jun. 2016.
- [6] M. Tonouchi, "Cutting-edge terahertz technology," *Nature Photon.*, vol. 1, pp. 97–105, Feb. 2007.
- [7] S. Koenig *et al.*, "Wireless sub-THz communication system with high data rate," *Nature Photon.*, vol. 7, no. 12, pp. 977–981, Dec. 2013.
- [8] H. Shams, M. J. Fice, K. Balakier, C. C. Renaud, F. V. Dijk, and A. J. Seeds, "Photonic generation for multichannel THz wireless communication," *Opt. Express*, vol. 22, no. 19, pp. 23465–23472, Sep. 2014.
- [9] H. J. Song and T. Nagatsuma, "Present and future of terahertz communications," *IEEE Trans. THz Sci. Technol.*, vol. 1, no. 1, pp. 256–263, Sep. 2011.
- [10] X. Pang *et al.*, "100 Gbit/s hybrid optical fiber-wireless link in the W-band (75–110 GHz)," *Opt. Express*, vol. 19, no. 25, pp. 24944–24949, Nov. 2011.
- [11] X. Li, J. Yu, J. Zhang, Z. Dong, F. Li, and N. Chi, "A 400G optical wireless integration delivery system," *Opt. Express*, vol. 21, no. 16, pp. 18812–18819, Aug. 2013.
- [12] X. Li, J. Yu, J. Xiao, Y. Xu, and L. Chen, "Photonics-aided over 100-Gbaud all-band (D-, W- and V-band) wireless delivery," in *Proc. 42nd Eur. Conf. Opt. Commun.*, Düsseldorf, Germany, 2016, Paper W.1.E.4.
- [13] J. Yu, X. Li, J. Zhang, and J. Xiao, "432-Gb/s PDM-16QAM signal wireless delivery at W-band using optical and antenna polarization multiplexing," in *Proc. Eur. Conf. Opt. Commun.*, Cannes, France, 2014, Paper We.3.6.6.
- [14] X. Li, Z. Dong, J. Yu, N. Chi, Y. Shao, and G. K. Chang, "Fiber-wireless transmission system of 108 Gb/s data over 80 km fiber and  $2 \times 2$  multiple-input multiple-output wireless links at 100 GHz W-band frequency," *Opt. Lett.*, vol. 37, no. 24, pp. 5106–5108, Dec. 2012.
- [15] X. Li, J. Yu, L. Zhao, K. Wang., W. Zhou, and J. Xiao, "1-Tb/s photonics-aided vector millimeter-wave signal wireless delivery at D-band," in *Proc. Opt. Fiber Commun. Conf.*, San Diego, CA, USA, Mar. 2018, Paper Th4D.1.
- [16] H. Shams *et al.*, "100 Gb/s multicarrier THz wireless transmission system with high frequency stability based on a gain-switched laser comb source," *IEEE Photon. J.*, vol. 7, no. 3, Jun. 2015, Art. no. 7902011.
- [17] S. Koenig *et al.*, "100 Gbit/s wireless link with mm-wave photonics," in *Proc. Opt. Fiber Commun. Conf.*, Anaheim, CA, USA, 2013, Paper PDP5B.4.
- [18] H. Shams, M. J. Fice, L. Gonzalez-Guerrero, C. C. Renaud, F. van Dijk, and A. J. Seeds, "Sub-THz wireless over fiber for frequency band 220–280 GHz," *J. Lightw. Technol.*, vol. 34, no. 20, pp. 4786–4793, Oct. 2016.
- [19] T. Kürner and S. Priebe, "Towards THz communications — status in research, standardization and regulation," *J. Infrared Milli. Terahz Waves*, vol. 35, no. 1, pp. 53–62, Jan. 2014.
- [20] A. J. Seeds, H. Shams, M. J. Fice, and C. C. Renaud, "Terahertz photonics for wireless communications," *J. Lightw. Technol.*, vol. 33, no. 3, pp. 579–587, Feb. 2015.
- [21] X. Yu *et al.*, "60 Gbit/s 400 GHz wireless transmission," in *Proc. Int. Conf. Photon. Switching*, Florence, Italy, 2015, pp. 4–6.
- [22] X. Yu *et al.*, "400-GHz wireless transmission of 60-Gb/s nyquist-QPSK signals using UTC-PD and heterodyne mixer," *IEEE Trans. THz Sci. Technol.*, vol. 6, no. 6, pp. 765–770, Nov. 2016.
- [23] S. Jia *et al.*, "Experimental analysis of THz receiver performance in 80 Gbit/s communication system," in *Proc. 41st Int. Conf. Infrared Milli. THz Waves*, Copenhagen, Denmark, 2016, Paper H5P.17.02.
- [24] S. Jia *et al.*, "80 Gbit/s 16-QAM multicarrier THz wireless communication link in the 400 GHz band," in *Proc. 42nd Eur. Conf. Opt. Commun.*, Düsseldorf, Germany, 2016, Paper W.1.E.5.
- [25] S. Jia *et al.*, "THz wireless transmission systems based on photonic generation of highly pure beat-notes," *IEEE Photon. J.*, vol. 8, no. 5, Oct. 2016, Art. no. 7905808.



- [26] S. Jia *et al.*, "THz photonic wireless links with 16-QAM modulation in the 375-450 GHz band," *Opt. Express*, vol. 24, no. 21, pp. 23777–23783, Oct. 2016.
- [27] S. Jia *et al.*, "120 Gb/s multi-channel THz wireless transmission and THz receiver performance analysis," *IEEE Photon. Technol. Lett.*, vol. 29, no. 3, pp. 310–313, Feb. 2017.
- [28] X. Yu *et al.*, "THz photonics-wireless transmission of 160 Gbit/s bitrate," in *Proc. 21st Optoelectron. Commun. Conf. Int. Conf. Photon. Switching*, Niigata, Japan, 2016, Paper PD1-2.
- [29] X. Yu *et al.*, "160 Gbit/s photonics wireless transmission in the 300–500 GHz band," *APL Photon.*, vol. 1, no. 8, Nov. 2016, Art. no. 081301.
- [30] X. Pang *et al.*, "Single channel 106 Gbit/s 16QAM wireless transmission in the 0.4 THz band," in *Proc. Opt. Fiber Commun. Conf.*, Los Angeles, CA, USA, 2017, Paper Tu3B.5.
- [31] S. Jia *et al.*, "0.4 THz photonic-wireless link with 106 Gbit/s single channel bitrate," *J. Lightw. Technol.*, vol. 36, no. 2, pp. 610–616, Jan. 2018.
- [32] S. Jia *et al.*, "A unified system with integrated generation of high-speed communication and high-resolution sensing signals based on THz photonics," *J. Lightw. Technol.*, vol. 36, no. 19, pp. 4549–4556, Oct. 2018.
- [33] S. Jia *et al.*, "Integrated dual-DFB laser for 408 GHz carrier generation enabling 131 Gbit/s wireless transmission over 10.7 Meters," in *Proc. Opt. Fiber Conf.*, 2019, Paper Th1C.2.
- [34] L. K. Oxenlewe *et al.*, "100s gigabit/s THz communication," in *Proc. Conf. Lasers Electro-Opt.*, 2018, Paper STu3D.1.
- [35] K. Liu *et al.*, "100 Gbit/s THz photonic wireless transmission in the 350-GHz band with extended reach," *IEEE Photon. Technol. Lett.*, vol. 30, no. 11, pp. 1064–1067, Apr. 2018.
- [36] K. Wang, X. Li, M. Kong, P. Gou, W. Zhou, and J. Yu, "Probabilistically shaped 16QAM signal transmission in a photonics-aided wireless terahertz-wave system," in *Proc. Opt. Fiber Commun. Conf.*, San Diego, CA, USA, 2018, Paper M4J.7.
- [37] X. Li *et al.*, "132-Gb/s photonics-aided single-carrier wireless terahertz-wave signal transmission at 450GHz enabled by 64QAM modulation and probabilistic shaping," in *Proc. Opt. Fiber Commun. Conf.*, San Diego, CA, USA, 2019, Paper M4F.4.
- [38] X. Pang *et al.*, "260 Gbit/s photonic-wireless link in the THz band," in *Proc. IEEE Photon. Conf., 29th Annual Conf. IEEE Photon. Soc.*, Hawaii, HI, USA, 2016, Paper PD1-2.
- [39] T. Ishibashi, Y. Muramoto, T. Yoshimatsu, and H. Ito, "Unitraveling-carrier photodiodes for terahertz applications," *IEEE J. Sel. Topics Quantum Electron.*, vol. 20, no. 6, pp. 79–88, Nov. 2014.
- [40] X. Pang *et al.*, "25 Gbit/s QPSK hybrid fiber-wireless transmission in the W-band (75–110 GHz) with remote antenna unit for in-building wireless networks," *IEEE Photon. J.*, vol. 4, no. 3, pp. 691–698, Jun. 2012.
- [41] B. Liu, X. Li, Y. Zhang, X. Xin, and J. Yu, "Probabilistic shaping for ROF system with heterodyne coherent detection," *APL Photon.*, vol. 2, no. 5, 2017, Art. no. 056104.
- [42] L. Zhang, M. Bi, S. Xiao, L. Liu, and Z. Zhou, "Channel estimation algorithm for interference suppression in IMDD-OQAM-OFDM transmission systems," *Opt. Commun.*, vol. 364, pp. 129–133, 2016.
- [43] L. Zhang *et al.*, "Nonlinearity-aware 200-Gbit/s discrete multi-tone transmission for C-band short-reach optical interconnects with a single packaged EML," *Opt. Lett.*, vol. 43, no. 2, pp. 182–185, 2018.
- [44] I. F. Akyildiz, C. Han, and S. Nie, "Combating the distance problem in the millimeter wave and terahertz frequency bands," *IEEE Commun. Mag.*, vol. 56, no. 6, pp. 102–108, Jun. 2018.

**Shi Jia** is currently working as a Postdoc with DTU Fotonik, Department of Photonics Engineering, Technical University of Denmark, Lyngby, Denmark. He obtained B.E. and MEng. degree in electrical and information engineering, both from Tianjin University, China, and received the Ph.D. degree in information and communication engineering in ministry of education key laboratory of opto-electronic information technology from Tianjin University, in 2017. He was a Visiting PhD student from 2015 to 2016 at DTU Fotonik sponsored by China Scholarship Council (CSC). He was a Postdoc at Zhejiang University from 2017 to 2018. His research interests cover the areas of high-speed optical communications, THz/microwave photonics, ultrahigh speed mm-wave/THz wireless communications, and optoelectronic oscillator (OEO). He has authored and coauthored around 50 publications in peer-reviewed scientific journals and international conferences. He has regularly served as a Designated Reviewer for the *Journal Optics Letters*, *Journal of Lightwave Technology* and *Optics Communications*.

**Lu Zhang** is currently a Research Associate Professor with the College of Information Science and Electronic Engineering at Zhejiang University. He received the bachelor degree from Southeast University in 2014 and the PhD degree from Shanghai Jiao Tong University in 2019. He was a Visiting PhD student from 2016 to 2017 at KTH Royal Institute of Technology sponsored by China Scholarship Council (CSC). Since 2018, he is a Visiting Research Engineer at KTH Royal Institute of Technology and Kista High-speed Transmission Lab of RISE AB. His research interests include ultra-fast THz communications, and fiber-optic communications, digital signal processing algorithms for optical and THz transmission systems.

**Shiwei Wang** is currently a PhD student with the College of Information Science and Electronic Engineering at Zhejiang University. He received his bachelor degree from the Harbin Institute of Technology, Weihai, China, in 2016. His research interests include THz/microwave photonics and THz communications.

**Wei Li**, biography not available at the time of publication.

**Mengyao Qiao**, biography not available at the time of publication.

**Zijie Lu**, biography not available at the time of publication.

**Nazar Muhammad Idrees**, biography not available at the time of publication.

**Xiaodan Pang** is currently a Senior Researcher with the Photonics Division, Department of Applied Physics at KTH. He is also a Group Member of the KTH/RISE Kista High Speed Transmission Lab, and a Guest Researcher at RISE Research Institutes of Sweden. He was a Staff Optical Engineer and a Research Fellow at Infinera Corporation Global R&D, Sweden from 2018 to 2020. He was a Researcher at KTH Optical Networks Laboratory (ONLAB), from 2017 to 2018. He works on high speed fiber-optic transmissions for short/long range systems. He has extensive experience in digital signal processing, multilevel modulations, radio-over-fiber, mm-wave and THz transmissions, coherent transmissions, Raman amplifications, system simulation, and laboratory instrumentation.

**Hao Hu**, biography not available at the time of publication.

**Xianmin Zhang**, biography not available at the time of publication.

**Leif K. Oxenlewe**, biography not available at the time of publication.

**Xianbin Yu** is currently a Research Professor with the College of Information Science and Electronic Engineering at Zhejiang University. He received his PhD degree in 2005 from Zhejiang University in China. From 2005 to 2007, he was a Postdoctoral Researcher at Tsinghua University, China. From 2007 to 2016, he was employed at DTU Fotonik, Technical University of Denmark, where he became an Assistant Professor in 2009 and was promoted to be a Senior Researcher in 2013. In 2016, he joined Zhejiang University as a Research Professor. His current research interests are in the areas of THz/microwave photonics, optical fiber communications, ultrahigh speed photonic wireless signal processing, and ultrahigh frequency wireless fiber access technologies.